

Torsional electromechanical quantum oscillations in carbon nanotubes

Tzahi Cohen-Karni^{1*}, Lior Segev^{1*}, Onit Srur-Lavi^{1*}, Sidney R. Cohen² & Ernesto Joselevich¹

¹*Department of Materials and Interfaces, and* ²*Chemical Research Support, Weizmann Institute of Science, Rehovot 76100, Israel.*

25 February 2006

Supplementary Information:

Table S1. Torsional mechanical characterization

Device:		D	E	F	G	H
Radius ^a (nm)	r	10 ± 1	10 ± 1	6 ± 1	6 ± 1	12.5 ± 1
Length ^a (nm)	ℓ	450 ± 20	450 ± 20	450 ± 20	450 ± 20	160 ± 10
Torsional spring constant (10 ⁻¹⁵ N·m)	κ	1.3 ± 0.1	1.9 ± 0.2	0.35 ± 0.3	0.32 ± 0.3	10 ± 2
Shear modulus ^b (GPa)	M	290 ± 75	420 ± 100	370 ± 140	340 ± 130	400 ± 80

^aFrom AFM topography. ^bAssigned to outermost wall only.

Table S2. Torsional electromechanical characteristics

Device:		A	B	C
Radius ^a (nm)	r	14 ± 1	13 ± 1	15 ± 1
Length ^a (nm)	ℓ	380 ± 20	300 ± 20	385 ± 20
Lever ^a (nm)	x	150 ± 20	135 ± 20	150 ± 20
Torsional spring constant ^b (10^{-15} N·m)	κ	11.2 ± 2.0	2.4 ± 0.5	5.2 ± 0.9
Shear modulus ^c (GPa)	M	750 ± 140	160 ± 30	290 ± 50
Torsion angle of failure ^b (deg)	ϕ_f	-	68 ± 3	45 ± 4
Torsional strength ^{b,c} (GPa)	τ	-	8 ± 2	9 ± 2
Observed maximum torque ^b (10^{-15} N·m)	$ \mathbf{T} ^{\max}_{\text{obs}}$	-	1.0 ± 0.3	2.0 ± 0.4
Calculated maximum torque ^c (10^{-15} N·m)	$ \mathbf{T} ^{\max}_{\text{cal}}$	-	1.0 ± 0.2	1.5 ± 0.3
Initial resistance (k Ω)	R^0	5800	500	3100
Observed oscillation periodicity (deg)	$\delta\phi_{\text{obs}}$	15 ± 4	12 ± 3	13 ± 4
Calculated minimal oscillation periodicity ^d (deg)	$\delta\phi_{\text{min}}$	16 ± 3	14 ± 2	14 ± 2
Estimated nanotube chirality ^e (deg)	θ	14 – 30	18 – 30	15 – 30
Attenuation factor	A	8.7	4.5	7.1
Initial activation energy ^f (meV)	E^0	0	16	14
Transmission probability ^f	$ t ^2$	0.01	0.11	0.025

^aFrom AFM topography. ^bFrom torque-torsion curves. ^cAssigned to outermost wall only.

^dCalculated for the maximal chirality $\theta = 30^\circ$. ^ePossible range within error margins. ^fHypothetical values assuming $E^0 = 0$ for metallic nanotubes and $E^0 = E_g^0/2 = \gamma_0 a_{C-C}/r$ for semiconducting ones.

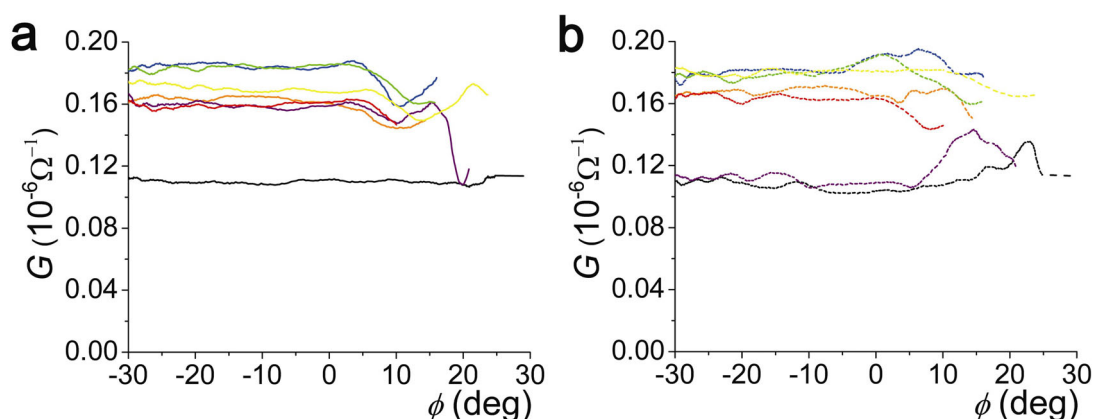


Figure S1. Torsional electromechanical response in the elastic regime for several consecutive actuations (following the rainbow order from red to purple). The pressing (**a**) and retracting (**b**) curves for the same actuations are displayed separately for clarity. The pressing purple curve ends with torsional failure. The purple retracting curve and both pressing and retracting black curves are already in the plastic regime. All the pressing curves show clearly the same reproducible oscillation in the elastic regime. Retracting curves follow the same behaviour, although presenting more noise and random shifts than the pressing curves, probably due to slack and adhesion. Overall, at least one oscillation is observed before torsional failure.

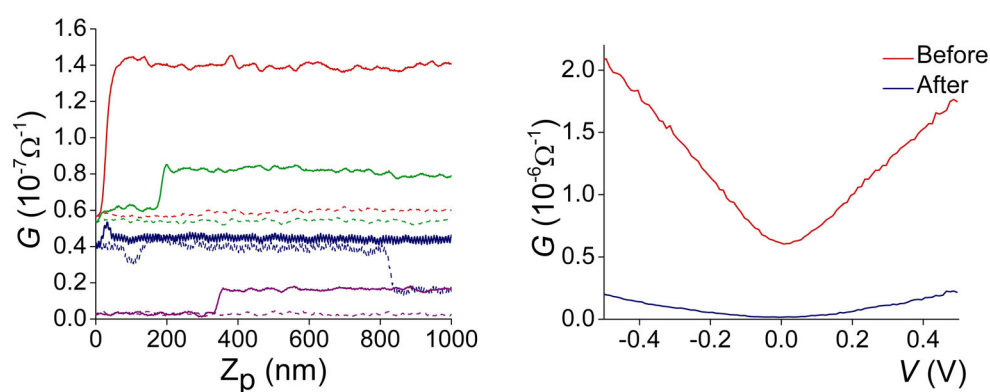


Figure S2. a Progressive torsional failure of a device in the plastic regime upon consecutive pressing-retracting loops. **b** Conductance $G(V)$ of a device before and after torsional failure.

Movie S1. (Available on-line) Elastic torsion of a nanotube-based NEMS by charging in a scanning electron microscope. This device was made with a very thin multiwalled carbon nanotube (nanotube diameter ~ 3-5 nm).

Methods

Materials and nanofabrication: Multiwalled carbon nanotubes (Ijjin Nanotech Co., Ltd.) were as-produced by arc-discharge, and dispersed in 1,2-dichloroethane or 1,2-dichlorobenzene by brief sonication prior to deposition. No surfactants, oxidizing agents, plasma or ozone were used during fabrication, to minimize damage and oxygen-doping. The torsional nanotube-based NEMS were produced as reported for similar devices^{5,9,23}. Briefly, the dispersion of multiwalled carbon nanotubes was spin coated on a thermally oxidized silicon wafer (Si<100>, boron-doped 0.005-0.025 Ω cm, oxide thickness: 1 μ m) containing an array of electron-beam lithographic alignment marks. The nanotubes were located by AFM imaging, and the electrodes and pedal were laid down on top of the selected nanotubes by electron-beam lithography (Nabity NPGS with JEOL 6400), followed by electron-beam evaporation of Cr (3-10 nm) and Au (100 nm) and lift-off with acetone. At this point, the samples were annealed at 400 °C in Ar for 5-10 minutes, then mounted onto a chip carrier, and wire-bonded. The SiO₂ underneath the nanotubes and pedals was etched in aqueous HF/NH₄F (1:6) for 5 minutes. Then, without drying the samples, the etching solution was consecutively replaced by water, ethanol and pressurized CO₂, from which they were critical-point-dried.

Measurements: AFM imaging, nanomanipulation and electromechanical measurements were done with a Veeco Multimode/Nanoscope IV using Nanoprobes FESP silicon tips (resonant frequency 70 kHz, nominal spring constant 1 N/m, recalibrated by the thermal noise method), except for the torsional mechanical characterization with variable lever distance (Fig 2b,c), which was done with closed-

loop NT-MDT EntegraTM AFM. Coupled electromechanical measurements (Fig. 3) were performed at room temperature under dry nitrogen, which reduces capillary tip-sample adhesion and minimizes thermal drifts. The chip-carrier with the sample was placed inside the AFM head, which was closed with a polydimethylsiloxane seal with an inlet for the dry nitrogen. The electrical measurements were done with a Perkin-Elmer DSP7280 lock-in amplifier, interfaced to the AFM and a computer with appropriate data acquisition cards. Samples were first imaged by tapping mode AFM. We then zoomed at the desired position on the pedal, and performed force-distance measurements while measuring the zero-bias differential conductance. The torsion angle and torque were monitored as explained in the text and Fig. 1d. The cantilevers were chosen to be relatively stiffer (1 N/m) than the pedals (0.04-0.2 N/m), so that torsion angles could be widely varied and monitored with relative accuracy, whereas the torque measurements are relatively less sensitive. A likely source of noise in the torque measurements, sometimes apparent as random narrow spikes, is the friction of the tip as it slides over asperities on the surface of the pedal during actuation. Due to the relative sensitivity of the torsion angle measurements with respect to the torque measurement, this noise may be assumed to have only a small effect on the actual torsion angle. SEM imaging (stills and movie) was performed with a Supra 55VP FEG LEO field-emission SEM in ultra-high vacuum, at acceleration voltage 5 kV, working distance 8 nm, and aperture 30 μm , and the beam current was about 0.5 nA.

Theoretical model

We shall first derive an expression for the torsion-induced bandgap change $\Delta E_g(\phi)$, following the graphical description shown in Fig. 4, and then describe how these changes are translated into torsion-induced changes in resistance (torsional piezoresistance). Due to the linearity and symmetry of the energy dispersion of graphene near the Fermi energy, the bandgap is equal to twice the energy k-gradient at

the Fermi energy $|\nabla_{\mathbf{k}} E|_{E_F}$ multiplied by the k-distance between the corner of the 1st Brillouin zone of graphene and the nearest subband. The latter is initially zero for metallic nanotubes and 1/3 of the subband spacing for semiconducting, and is shifted by the torsion-induced shift of the Brillouin zone corner perpendicular to the subbands. Hence, the bandgap is given by eq. S1, where $p = 0, 1$ or -1 is given by the crystallographic indices, $n - m = 3q + p$, and Δj is an integer number corresponding to the change in the quantum number associated with the nearest subband before and after twisting. Substituting all the terms by these definitions leads to eq. S2. Since the initial bandgap is $E_g^0 = |p|\gamma_0 a_{C-C}/r$, the bandgap change with torsion is given by eq. S3. This expression describes the period and the amplitude of the band gap oscillations, $\delta\phi = a_{C-C} \ell / r^2 \sin(3\theta^0)$ and $\Delta E_g^{max} = 3\gamma_0 a_{C-C}/2r$, respectively, displayed in Fig. 4.

$$E_g(\phi) = 2|\nabla_{\mathbf{k}} E|_{E_F} \left| p\delta k/3 + \Delta j\delta k + \Delta k_F^c(\phi) \right| \quad (S1)$$

$$E_g(\phi) = \frac{3\gamma_0 a_{C-C}}{r} \left| \frac{r^2 \sin 3\theta^0}{a_{C-C}\ell} \phi + \Delta j + \frac{p}{3} \right| \quad (S2)$$

$$\Delta E_g(\phi) = \frac{3\gamma_0 a_{C-C}}{r} \left[\frac{r^2 \sin 3\theta^0}{a_{C-C}\ell} \phi + \Delta j \right] \quad (S3)$$

The overall resistance of the torsional nanotube-based NEMS arises from the series contributions from the two suspended nanotube segments on both sides of the pedal, which are simultaneously twisted at opposite angles ϕ and $-\phi$, and from the metal-nanotube contacts R_c , as given by eq. S4. Assuming ballistic conduction, the resistance of each twisted segment $R_t(\phi)$ can be modelled following the Landauer-Büttiker formula, eq. S5, where $F(E)$ is the Fermi-Dirac function, $T(E)$ is the transmission probability, and N is the number of channels. At low-bias, the number of channels accessible for conduction is $N=2$, corresponding to wavevectors \mathbf{k} and $-\mathbf{k}$. We assume that electrons with energies within the bandgap are scattered (eq. S6), whereas those with energies below the valence band edge E_v or above the conduction band edge E_c can

flow across the nanotube with a transmission probability $|t|^2$ (eq. S7). We first assume the simplest case of an intrinsic (undoped) nanotube without Schottky barriers, and then make corrections for the other cases. In the first case, the Fermi energy is found exactly in the middle of the bandgap, so the solution to the Landauer-Büttiker formula (eq. S5) is eq. S8. By inserting this solution into eq. S4 for the two oppositely twisted nanotube segments, the overall resistance is given by eq. S9. This can be rearranged into the equations given in the text, where the initial activation energy is $E^0 = E_g^0/2$ and its torsion-induced change is $\Delta E(\phi) = \Delta E_g(\phi)/2$.

$$R(\phi) = R_c + R_t(\phi) + R_t(-\phi) \quad (\text{S4})$$

$$\frac{1}{R_t(\phi)} = G_t = N \frac{2e^2}{h} \int_{-\infty}^{\infty} \left(-\frac{\partial F}{\partial E} \right) T(E) dE \quad (\text{S5})$$

$$T(E_v < E < E_c) = 0 \quad (\text{S6})$$

$$T(E < E_v) = T(E > E_c) = |t|^2 \quad (\text{S7})$$

$$G_t = \frac{4e^2|t|^2}{h} \int_{-\infty}^{E_F - E_g/2} \left(-\frac{\partial F}{\partial E} \right) dE + \frac{4e^2|t|^2}{h} \int_{E_F - E_g/2}^{\infty} \left(-\frac{\partial F}{\partial E} \right) dE = \frac{8e^2|t|^2}{h} \cdot \frac{1}{e^{\frac{E_g}{2k_B T}} + 1} \quad (\text{S8})$$

$$R(\phi) = R_c + \frac{h}{8e^2|t|^2} \left[e^{\frac{E_g^0 + \Delta E_g(\phi)}{2k_B T}} + 1 \right] + \frac{h}{8e^2|t|^2} \left[e^{\frac{E_g^0 + \Delta E_g(-\phi)}{2k_B T}} + 1 \right] \quad (\text{S9})$$

Now we address the effects of doping and Schottky barriers. If the nanotube is lightly doped with a Fermi energy shift ΔE_F^0 , then the result of the Landauer-Büttiker formula (eq. S5) is eq. S10, and the resistance of each twisted nanotube segment is given by eq. S11. This makes the analytical expression for the relative change in resistance rather complicated. However, if ΔE_F^0 is comparable to $E_g/2$, then the right term in eq. S10 becomes negligible, and the relative change in resistance becomes similar to the equations provided in the text, where $E^0 = E_g/2 - |\Delta E_F^0|$. This can

significantly increase the attenuation factor A , but, due to the bandgap changes with torsion, an electromechanical effect could still be observed, even if E^0 is very small or negative. If the current is limited by thermionic emission through a Schottky barrier, then the transmission probability becomes zero below the zero-bias barrier height Φ_{B0} , so the solution has the same form as given in the text, but $E^0 = \Phi_{B0}$. A more complicated case is if doping is so heavy that the Fermi energy shift is larger than the inter-subband energy δE , so that $|\Delta E_F^0| > E_g/2 + n\delta E$, where n is an integer number. In this case, more than one subband contributes to conduction. Since the energy of all the subbands is shifted by torsion, an electromechanical effect might still be observed if only a few subbands participate, but not if doping is too heavy.

$$G_t = \frac{4e^2|t|^2}{h} \left(\frac{1}{e^{\frac{E_g - |\Delta E_F^0|}{2k_B T}} + 1} + \frac{1}{e^{\frac{E_g + |\Delta E_F^0|}{2k_B T}} + 1} \right) \quad (\text{S10})$$

$$R_t(\phi) = \frac{h}{8e^2|t|^2} \left[\frac{e^{\frac{E_g^0 + \Delta E_g(\phi)}{k_B T}} - 1}{\cosh\left(\frac{\Delta E_F^0}{k_B T}\right) e^{\frac{E_g^0 + \Delta E_g(\phi)}{2k_B T}} + 1} + 2 \right] \quad (\text{S11})$$

In summary, in the ideal case of an intrinsic nanotube, the initial activation energy is half the bandgap, $E^0 = E_g/2$. If the nanotube is doped, the activation energy is lowered by the Fermi energy shift to $E^0 = E_g/2 - |\Delta E_F^0|$, leading to large attenuation, but still observable changes in resistance. If the current is limited by a Schottky barrier, then $E^0 = \Phi_{B0}$ (the barrier height). If the Fermi energy shift due to doping is larger than the inter-subband energy ($\Delta E_F^0 > \delta E \approx 50$ meV), the picture is complicated by the participation of more than one subband in the conduction, but since the energies of all the subbands are shifted by torsion, there can still be an electromechanical effect. In any case, the torsion-induced change in activation energy is half the bandgap change, $\Delta E(\phi) = \Delta E_g(\phi)/2$.

Lastly, we should note that the assumption of ballistic conduction, which is consistent with the hyperbolic shapes of the experimental $G(V)$ curves (Fig. 2b), makes it easier to model the torsional piezoresistance, but ballistic conduction is not a necessary condition for the torsional electromechanical oscillations, as long as there is a modulation of the band gap, which should not be affected by scattering.

Possible effect of tension vs. torsion

To address the possible effect of tension vs. torsion, we calculate the uniaxial strain along the nanotube, and compare its expected electromechanical effect with that of torsional strain. An upper limit to the uniaxial strain is calculated by assuming that all the force exerted on the pedal leads to stretching of the nanotube outer wall, neglecting the force that is compensated by the bending rigidity of all the nanotube walls. In this case, each suspended segment of nanotube on either side of the pedal can be assumed to be straight and stretched down by an angle α from the initial horizontal position to a length $\ell + \Delta\ell$. This directly leads to eq. S12, where the uniaxial strain is $\sigma = \Delta\ell / \ell$. The force F_z exerted by the tip on the pedal is countered by the normal components of the tension force F_t along the two nanotube segments, as expressed in eq. S13. The tension is related to the uniaxial strain by the tensile Young's modulus Y and the cross-section area A_{cs} , as in eq. S14. Combining eqs. S12-S14 leads to eq. 15. For relatively small uniaxial strains $\sigma \ll 1$, the uniaxial strain can be given by eq. 16.

$$\cos \alpha = \frac{\ell}{\ell + \Delta\ell} = \frac{1}{1 + \sigma} \quad (\text{S12})$$

$$F_z = 2F_t \sin \alpha \quad (\text{S13})$$

$$F_t = YA_{cs}\sigma \quad (\text{S14})$$

$$F_z = \frac{2YA_{cs}\sigma^{3/2}(2 + \sigma)^{1/2}}{1 + \sigma} \quad (\text{S15})$$

$$\sigma = \frac{1}{2} \left(\frac{F_z}{YA_{cs}} \right)^{2/3} \quad (\text{S16})$$

The measured normal force can be retrieved back from the torque-torsion data (Fig. 3 and table S2) as $F_z = |\mathbf{T}|/x$. The cross-section area of the outer wall is $A_{cs} = 2r\delta r$ and $Y = 1$ TPa. For example, from the maximum observed torque in device B (in which 5 oscillations are observed) the maximum normal force is 15 nN, which corresponds to a uniaxial strain of $\sigma = 0.007$. This is one order of magnitude smaller than the maximum torsional strain for the same experiment, $\xi = 0.06$. The overall shift of the corner of the 1st Brillouin zone perpendicular to the subbands, following the Yang-Han model⁸, is given by eq. S17, where ν is the Poisson ratio (which in this case can be neglected due to the presence of the inner walls). The maximum shift that can be expected from tension for $\sigma = 0.007$ is $\Delta k_F^c = 5 \times 10^7 \text{ m}^{-1}$, which is one order of magnitude smaller than the maximum shift from torsion for $\xi = 0.06$, $\Delta k_F^c = 4.3 \times 10^8 \text{ m}^{-1}$, and is smaller than the subband spacing $\delta k = 1/r = 8 \times 10^7 \text{ m}^{-1}$, although not negligible. Hence, we can conclude that the maximum possible electromechanical effect of tension in our devices might not be completely negligible, but it should be monotonical and not oscillatory, so it would be difficult to detect. If we considered the bending rigidity of all the nanotube walls, which could be significant compared to the tensile rigidity of the outer wall, then the maximal effect of tension would be even smaller.

$$\Delta k_F^c = \frac{1}{a_{C-C}} \left[(1 + \nu)\sigma \cos 3\theta^0 + \xi \sin 3\theta^0 \right] \quad (\text{S17})$$